Supplementary Information

Natural fibre based sustainable and high-performance platform for electrochemical sensors

Nachiket Aashish Gokhale[1,2,3], Chiranjeevi Srinivasa Rao Vusa[1,2], and Siddhartha Panda[1,2,3*]

[1] Samtel Centre for Display Technologies, Indian Institute of Technology Kanpur, Kanpur, 208016, India

[2] National Centre for Flexible Electronics, Indian Institute of Technology Kanpur, Kanpur, 208016, India

[3] Department of Chemical Engineering, Indian Institute of Technology Kanpur, Kanpur, 208016, India

*** Corresponding author**: spanda@iitk.ac.in,

ORCHID IDs

Nachiket Aashish Gokhale: 0000-0001-9467-5911

Chiranjeevi Srinivasa Rao Vusa: 0000-0002-7177-6792

Siddhartha Panda: 0000-0001-9131-4264

S1: Sweat preparation protocol

Table S1: Composition of sweat [1]

CH_4N_2O (urea)	1 g l^{-1}
$C_3H_6O_3$ (lactic acid)	1 ml l^{-1}
KCl	1 g l^{-1}
KH_2PO_4	245 mg l^{-1}
NaCl	7.5 g l^{-1}
Na_2HPO_4	1.44g l^{-1}

S2: Inventory for sugarcane production:

Table S2: input and output inventory for sugarcane production (basis 1ton sugarcane)[2]

Inputs	**Amount**	**Unit**
Ammonium nitrate	0.134	kg
Ammonium sulphate	0.133	kg
Caneseed	136.04	kg
Carbon dioxide	599.43	kg
Lime	5.25	kg
Tractor	3.97	t × km
Diammonium phosphate	0.156	kg
Diesel	2.13	kg
Land occupation	149	m^2 × year
Phosphate (P_2O_5)	38.3	g
Diammonium phosphate, as P_2O_5	0.34	kg
Potassium chloride, as K_2O	1.56	kg
Potassium nitrate, as P_2O_5	17.04	g
Potassium nitrate, as N	8.38	g
Potassium sulphate, as P_2O_5	17.04	g
Single superphosphate, as P_2O_5	227.27	g
Triple superphosphate	123.58	g
Urea	397.72	g
Freshwater	68.49	m^3

Outputs		
Sugarcane	1000	kg
Ammonia	51.12	g
Carbon dioxide	4.26	kg
Carbon monoxide	38.34	g
Methane	96.56	g
Nitrate	21.01	g
Nitrogen	323.76	g
Nitrogen oxides	452.98	g
Nitrous oxide	200	g
NMVOC	218.68	g
Particulates, > 2.5 and < 10 µm	10.22	g
Phosphorus	3.97	g
Sulphur oxides	50.8	g

S3: Optimization of deposition thickness, adhesion test:

Optimization of deposition thickness:

Different thicknesses of 5, 10, 25, 50, 100, and 250 nm of gold were deposited on the sugarcane skin to investigate the influence of deposition thickness on the performance of the chip. The chips with 5, 10, 25 nm of deposition thickness deteriorated while performing cyclic voltammetry in 10mM $K_4[Fe(CN)_6]$ and $K_3[Fe(CN)_6]$ in 100 mM KCl. 50 nm thickness deposition gave stable response for 20 cycles as can be seen in Figure S3A. Similar stable response was also observed in 100 and 250 nm thick deposition. Increasing the deposition thickness will result in the loss of nano features on the SugarcaneSens hence, reducing the ECSA and the cost of production will also increase. Thus, an optimum thickness of 50 nm was chosen for all the subsequent experiments.

Adhesion test:

The adhesion test was performed according to ASTMD3359 protocol on the SugarcaneSens [3]. Briefly, skins of sugarcane were deposited with 50 nm of gold and scratches were made on them. An ‘X’ shaped scratch was made for test A and lattice patterned scratches were made for

test B. pressure sensitive adhesive tape was applied over both the strips and then removed. The adhesion is evaluated by comparison with the descriptions and illustration given in the protocol.

In both the test A and B, there was a trace removal of the coating (< 5%), hence the coating will be graded as type 4 coating.

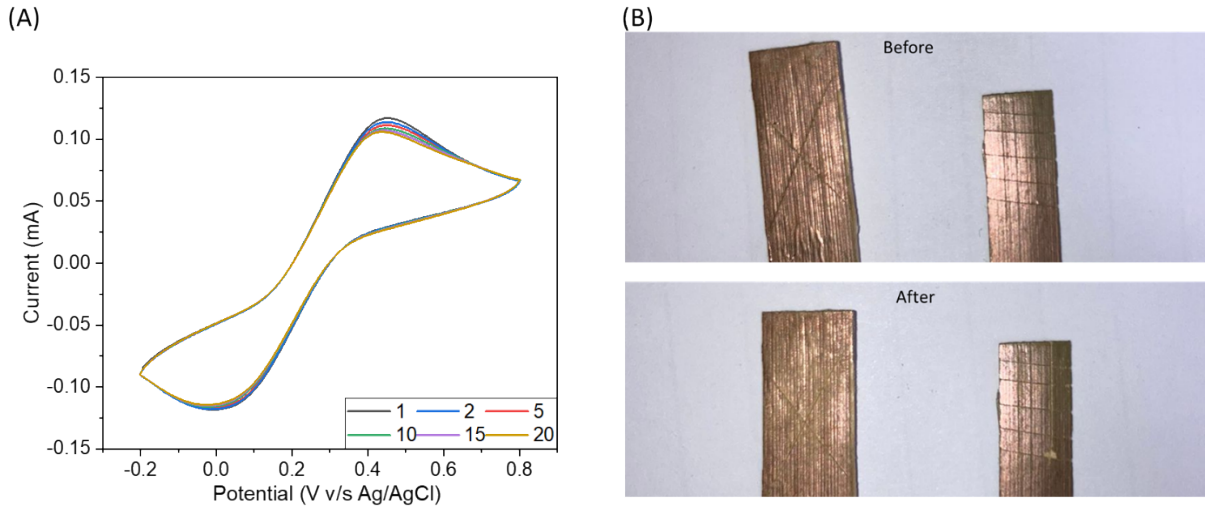

Figure S3: (A) multiple cycles of CV for 50 nm Au deposited in 10 mM $K_4[Fe(CN)_6]$ and $K_3[Fe(CN)_6]$ in 0.1M KCl at a scanrate of 50 mV s^{-1} and (B) images of adhesion test, before and after scratching

S4: AFM of CER and PET

The 3D image of AFM and its section graph for CER and PET is attached in figure S4A and S4B respectively.

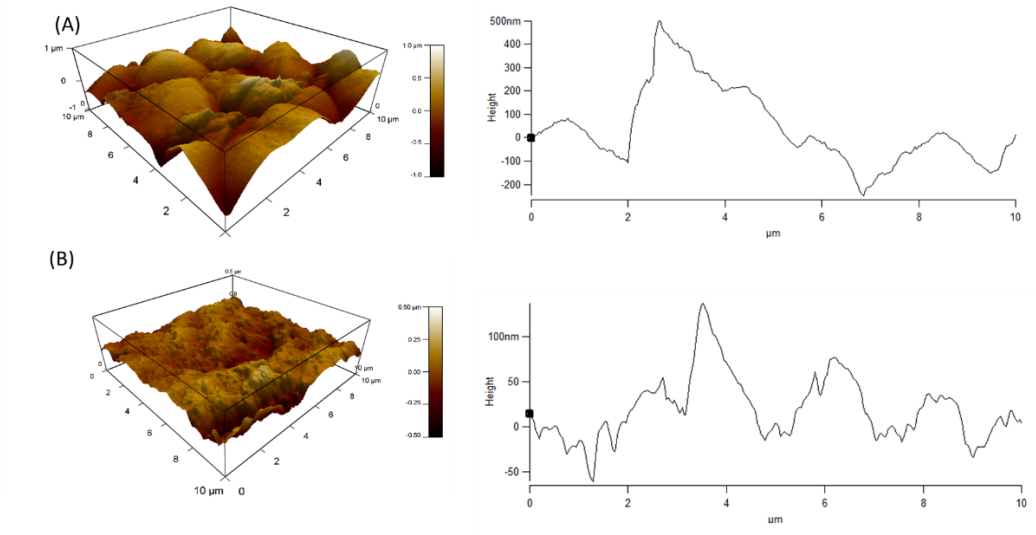

Figure S4: 3D image and section graph of AFM for (A) CER and (B) PET substrate.

S5: ECSA measurements:

The peaks in CV correspond to the oxidation and reduction of Au and Au-oxides.

The ECSA of the WE for SSE, CER and PET chips were calculated using the charge associated with the reduction of gold oxide by integration, which is proportional to the real active surface area of the gold surface.

Charge (Q) = $\frac{Area\ under\ the\ peak}{Scan\ rate} = \frac{1.11 * 10^{-4}}{0.05}$ = 0.222mC,

which is equal to 222 μC

ECSA = $\frac{Q\ (in \mu C)}{Q_o} = \frac{222}{390}$ = **0.569 cm²**

RF = $\frac{Electrochemical\ surface\ area}{Geometrical\ area} = \frac{0.605}{0.0707}$ = **8.05**

Note: The Q_o 390 μC cm^{-2} value has been suggested for polycrystalline gold.

Though shorter and broader reduction current peaks were observed at a lower concentration (50 mM H_2SO_4) than at a higher concentration (500 mM H_2SO_4), the peak area is almost same. Hence there is no change in the ECSA. There are more chances of errors in area calculation of broader peaks, hence 500mM H_2SO_4 is chosen as the optimum concentration. There is a shift in the peak position, this is due to the change in pH.

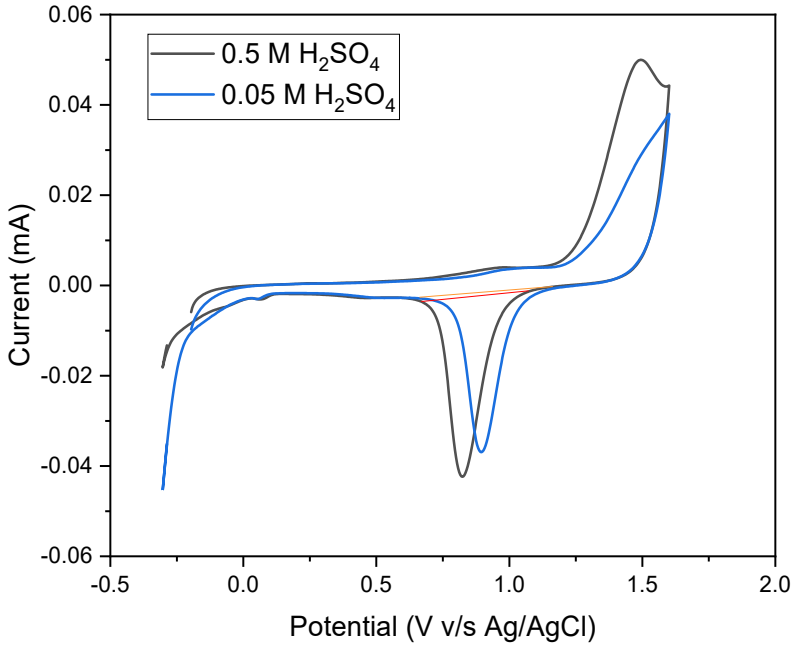

Figure S5: CV response of SSE in 0.05 M and 0.5 M H_2SO_4

S6: Images of contact angle measurements:

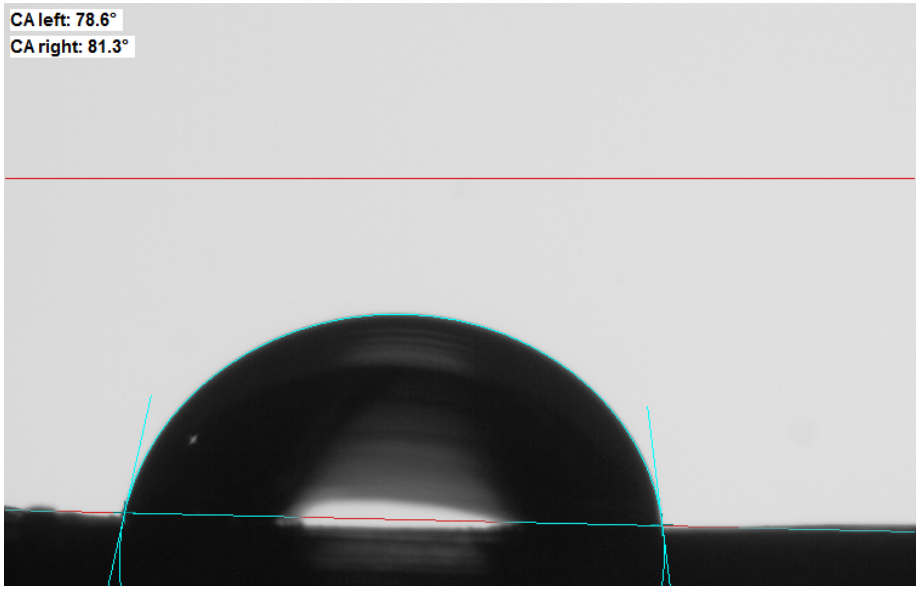

Figure S6: Image for the contact angle measurement of the working electrode of the SSE chip with water

Casie Baxter Model of surface wettability:

Cassie-Baxter surface wettability model explains the relationship between contact angle and surface roughness. The contact angle of a liquid droplet increases with the fraction of air (σ) entrapped by the surface topography (equation 1). [4]

$$\sigma = (\cos(\theta_r) - cos(\theta))/(cos(\theta) + 1) \quad \ldots(1)$$

where θ_r is the contact angle of the modified surface and θ is the contact angle of the planar electrode.

The contact angle of the SugarcaneSens is more than that of planar electrode and this can be attributed to the surface roughness of the electrode using Casie Baxter model.

S7: Shelf-life studies

The images of stored electrodes are shown in the Figure S6. The effect of temperature fluctuations was also studied by storing the electrode in a refrigerator at 3 ^{o}C for 7 days. ECSA was measured and a negligible change of 4% was observed.

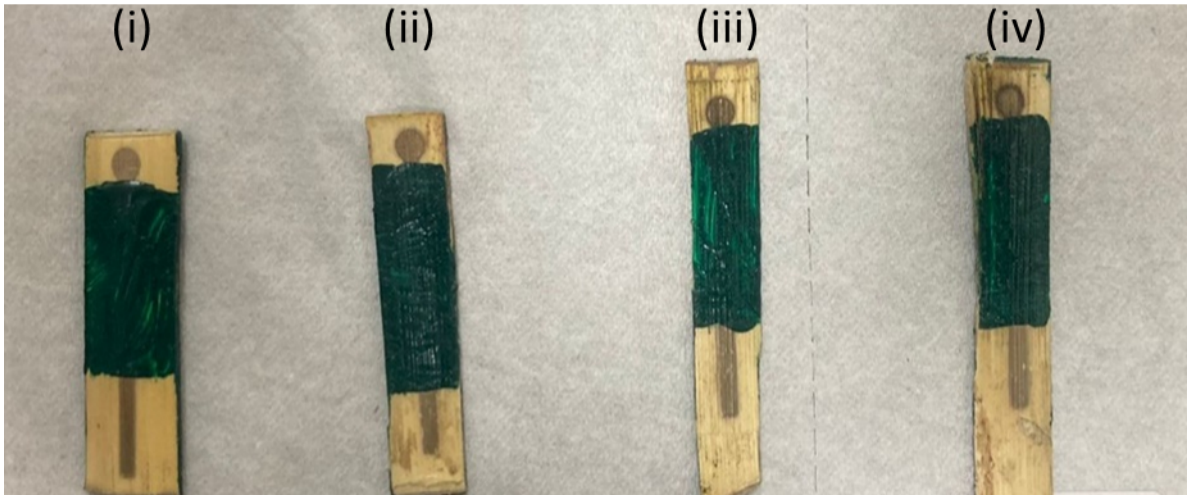

Figure S7: images of the SSE (i) fresh, (ii) 1-year-old (iii) 2-year-old and (iv) 1.5-year-old after dipped in liquid.

S8: CV for various concentrations of glucose in 0.1M KOH sweat.

As can be seen in the figure S7, a peak at ~0.5 V is observed due to electro-oxidation of glucose. The peak current is increasing with increase in glucose concentration. Hence, 0.5 V is chosen as the potential for amperometry. The potential was also varied to 0.45 and 0.55V, but no direct relationship between current and concentration was observed for 0.45V and similar issue was observed for 0.55 V.

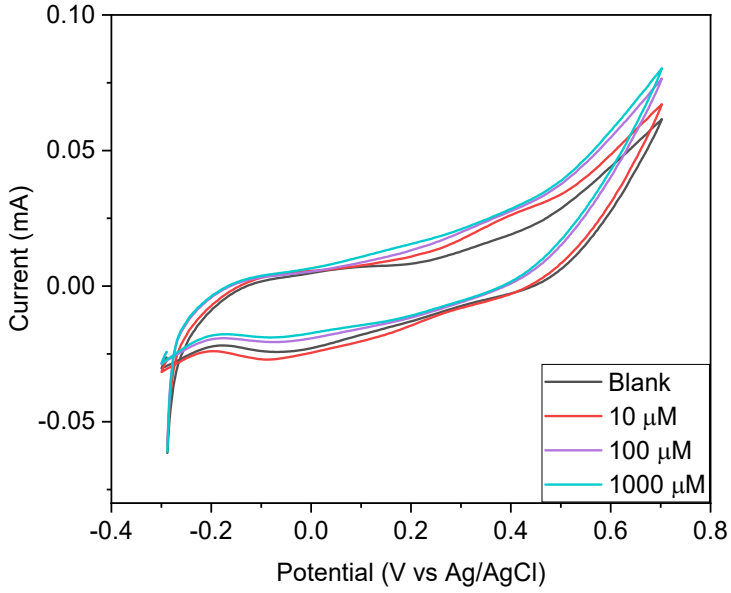

Figure S8: CV for SSE in blank and various concentrations of glucose in 0.1 M KOH sweat at 50 mV s^{-1}

S9: Interference of glucose from sugarcane skin in measurements:

Quantitative and qualitative analysis is performed using Fehling's test and commercial glucometer respectively.

For qualitative analysis, Fehling's solution A was prepared by dissolving 7.0 g of CuSO4.7H2O in 100 ml H2O. Fehling's solution B was prepared by dissolving 24.0 g of KOH and 34.6 g of potassium sodium tartarate in 100 ml. Equal volumes of A and B solution just before use.

1 ml of Fehling's reagent was mixed with test solution and heated in boiling water bath for 2-3 min.

SugarcaneSens chip was dipped in 5 ml of water to test the effect of glucose diffusion from the SugarcaneSens. 1 ml of solution was taken out after day 1 to quantitively check the diffusion of glucose in solution. The results were compared with (i) blank solution and (ii) 0.1 mM glucose. The formation of brownish deposit as seen in (ii) of figure S8, confirms the presence of glucose. No such visible change in the colour was observed for the solution taken out after 1 hr (figure S8, (iii)), indicating that there is a negligible diffusion after 1 hr of water exposure. However, after day 2, some brownish deposits were observed (figure S8, (iv)).

The extent of glucose diffusion was quantified using commercial glucometer (Accucheck Active by Roche, Germany). The least count of this device is 1000 µM. Even after 7 days, the concentration of glucose in the solution was not measurable (< 1000 µM).

The total time for sensing glucose using SugarcaneSens is 1 minute, and the sensing range is 1 µM to 2000 µM. Hence, we can conclude that the effect of glucose diffusion into the system has negligible effect on glucose sensing.

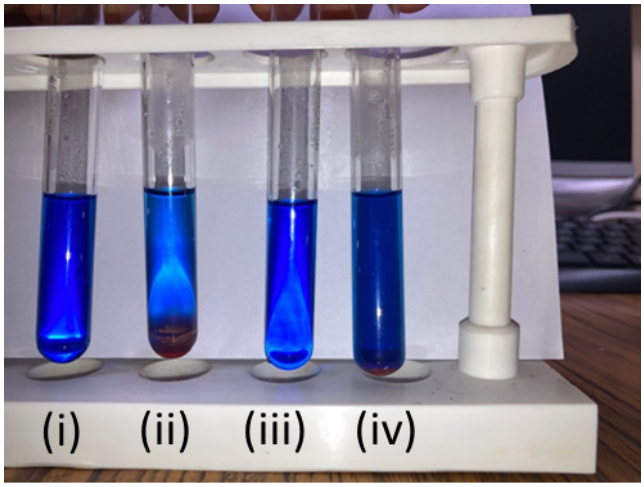

Figure S9: Results of Fehling's test in (i) blank, (ii) 0.1 mM glucose in water, (iii) SugarcaneSens after 1 hr and (iv) in SugarcaneSens after 2 days

The diffusion of glucose from Sugarcane Sens in the solution is ~100 nM/min. It takes just 1 minute to sense glucose with this device and the working range of this device is 1 µM to 2000 µM with a LOD of 500 nM. Hence, the glucose contained in sugar cane is not playing a role in the detection.

S10: Amperometry response for glucose sensing experiments

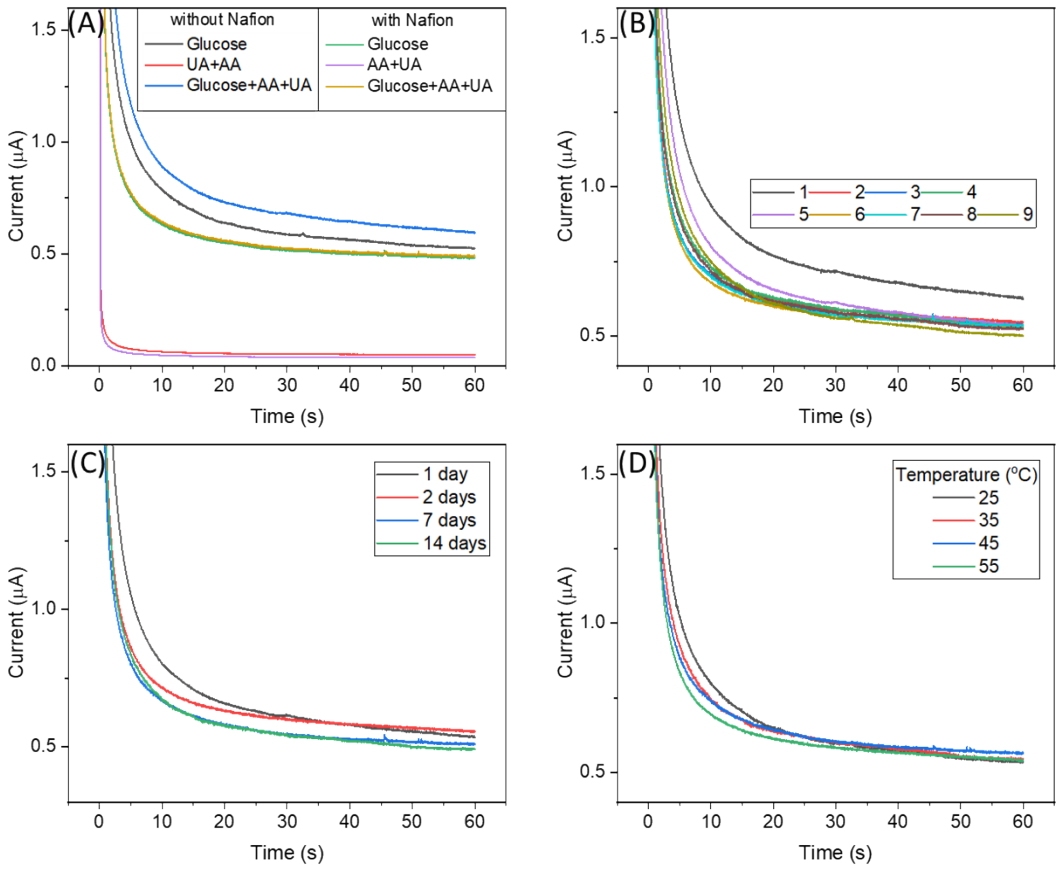

Figure S10: Amperometry response for (A) interference study, (B) reusability test, (C) time stability analysis and (D) effect of temperature on glucose sensing.

S11: Extent of heavy metals in SugarcaneSens

The presence of heavy metals in SugarcaneSens was quantitatively and qualitatively examined using inductively coupled plasma mass spectrometry (ICPMS).

SugarcaneSens chip was dipped in DI water for 2 days and the sample was tested for Cd, Pb and As using ICPMS. The results showed that none of them diffused in water on day 1. On day 2 the concentration of As was 0.165 ppb, and Cd and Pb was <0.001 ppb.

Table S11: ICPMS data for standard solution, blank and SugarcaneSens.

Sample Name	As Conc. [ppb]	Cd Conc. [ppb]	Pb Conc. [ppb]
BLANK	0	0	0
Standard-100	98.9717005	98.6138791	97.023346
Standard-200	200.593123	201.145253	197.084523
Standard-300	303.334425	300.966453	299.193972
Standard-400	399.701095	398.389648	402.270239
Standard-500	498.20688	500.527533	504.028948
SugarcaneSens- Day 1	<0.001	0	0
SugarcaneSens- Day 2	0.16508617	<0.001	<0.001

S12: Optimization of deposition potential and time for cadmium detection

The deposition potential for the Cd^{2+} detection was optimized by varying the potential from -0.9 V to -1.8 V. The stripping current for 100 nM Cd^{2+} (after baseline correction) is plotted in Figure S12A, and an optimum potential of -1.5 V is obtained. The deposition time was optimised using the optimised potential and the striping current is plotted in Figure S12B.

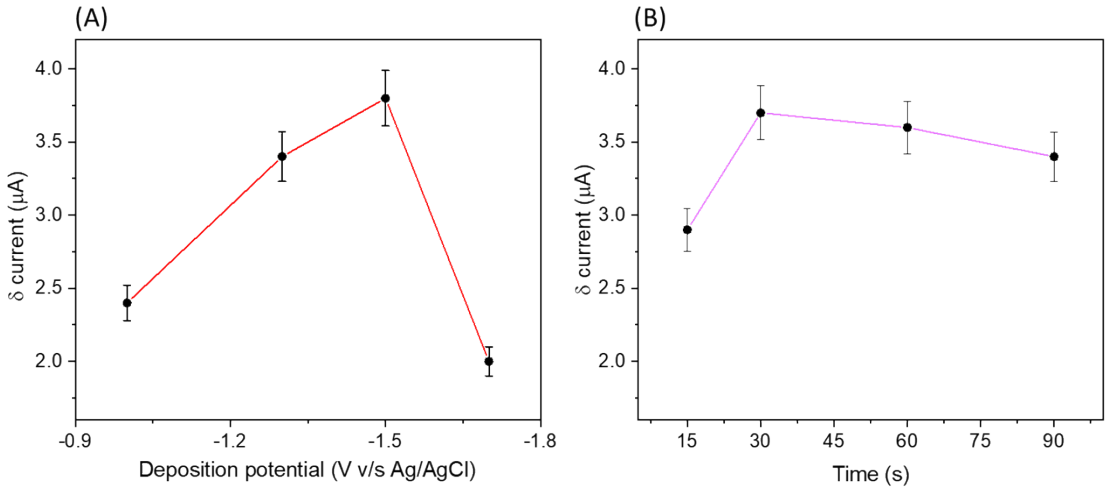

Figure S12: Stripping current for 10 nM Cd^{2+} in 4.5pH acetate buffer for (A) different values of deposition potential and (B) different values of deposition time using the optimised potential.

S13: Anodic Stripping Voltammograms for cadmium detection

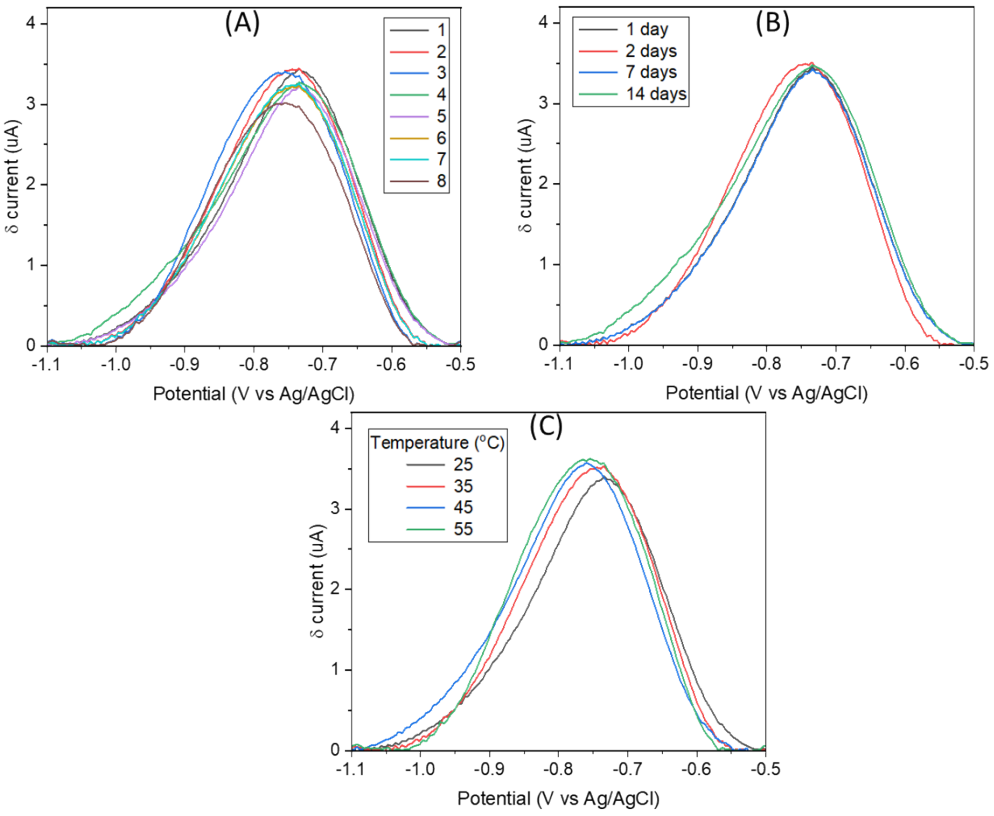

Figure S13: ASV curves of Cd^{2+} detection for (A) reusability test performed using the same chip several times, (B) time stability analysis and (C) effect of temperature on cadmium sensing.

References:

(1) Baker, L. B. Physiology of Sweat Gland Function: The Roles of Sweating and Sweat Composition in Human Health. *Temperature* **2019**, *6* (3), 211–259. https://doi.org/10.1080/23328940.2019.1632145.

(2) Srivastava, S. K.; Kumar, R.; Singh, R. P. *Extent of Groundwater Extraction and Irrigation Efficiency on Farms under Different Water-Market Regimes in Central Uttar Pradesh*; Vol. 22.

(3) ASTM international. D3359-Standard Test Methods for Measuring Adhesion by Tape Test. **2009**. https://doi.org/10.1520/D3359-09E02.

(4) Cassie, A. B. D.; Baxter, S. Wettability of Porous Surfaces. *Transactions of the Faraday Society* **1944**, *40*, 546. https://doi.org/10.1039/tf9444000546.